



Semnan University

Mechanics of Advanced Composite Structures

journal homepage: <http://MACS.journals.semnan.ac.ir>

Higher-order Displacement Model for Cylindrical Bending of Laminated and Sandwich Plates Subjected to Environmental Loads

N.S. Naik*, A.S. Sayyad

Research Scholar, Department of Civil Engineering, SRES's Sanjiv ani College of Engineering, Savitribai Phule Pune University, Kopargaon-423603, Maharashtra, India

KEYWORDS

Cylindrical bending
Laminated
Sandwich
Shear deformation
Normal deformation

ABSTRACT

In this research article, thermal and hygrothermal stress analysis of composite layered and sandwich plate having one dimension infinitely long and simply supported on the edges is presented using a new fifth-order theory. The proposed theory considers, the effect of thickness stretching. The present theory uses a polynomial shape function to account for transverse shear deformation using the expansion of thickness up to a fifth-order while to consider the effect of thickness stretching the derivative of shape function is used in the transverse displacement. In this theory, the shear strain variation is assumed to be parabolic across the thickness. The present displacement field satisfies zero shear stress condition both at the top and bottom surfaces and avoids the use of a shear correction factor. The governing equations are derived using the virtual work principle. For solution of problem, Navier's solution technique is used. The results generated using the present theory are compared with the existing elasticity solution wherever it is available. However, many results for the cylindrical flexural analysis of laminated and sandwich plates subjected to environmental loading are presented for the first time in this paper.

1. Introduction

Composite material is characterized by its low density, high-modulus, high strength and low weight and its flexibility to tailor it as per the structural requirements. Because of these important properties it is widely used in many branches of engineering viz. civil engineering, aerospace engineering, mechanical engineering etc. Composite material during its life span has to carry different types of loadings, like mechanical load and environmental loads (Thermal/hygrothermal). Environmental loads like temperature and moisture result in degradation of the properties and reduction in the strength. Hence, considering the use of composite material in important applications and effect of environmental loads on it, it is necessary to analyze composite structures for mechanical as well as environmental loads.

The literature available on cylindrical bending analysis of composite laminates subjected to environmental loading is scarce. The review of

available literature on the development of theories used to analyze beams, plates and shell is documented by Timoshenko and Woinowsky-Krieger [1], Todhunter and Pearson [2] and Carrera et al. [3]. Pagano [4-6] developed benchmark exact solution for 1D and 2D bending analysis of laminated composite plates and sandwiches. Kirchhoff [7] developed the simplest theory (Classical Plate Theory i.e. CPT) ignoring the shear deformation effect. CPT cannot be applied to plates having a considerable thickness and in which shear deformation effect is significant. To overcome the drawback of CPT, first time Mindlin [8] developed first order shear deformation theory (FSDT) assuming constant shear strain across the thickness. Hence FSDT does not satisfy zero shear stress conditions at the top and bottom surfaces of the plate and needs a shear correction factor. The limitations of CPT and FSDT initiated the need of shear deformation theories with a higher order. Sayyad and Ghugal [9-11] used exponential theory for the study of flexural and vibrational analysis of

* Corresponding author. Tel.: +91-9763567881
E-mail address: attu_sayyad@yahoo.co.in

thick plates. Ghugal and Dahake [12] developed a trigonometric shear deformation theory using the sinusoidal function for the analysis of deep beams carrying parabolic load. Sayyad and Ghugal [13] studied the flexural behavior of soft-core sandwich beams using trigonometric shear deformation theory. Sayyad and Ghugal [14] presented an n^{th} order theory with consideration of the shear deformation effect for the cylindrical bending analysis of composites. Sayyad and Ghugal [15] also studied bending, buckling and free vibrations of homogeneous beams using single variable refined beam theories. Shinde and Sayyad [16] analyzed isotropic, functionally graded, laminated and sandwich beams using a quasi-3D polynomial shear deformation theory. Sayyad and Ghugal [17] investigated bending, buckling, and free vibration responses of functionally graded material beams using hyperbolic shear deformation theory. Recently Sayyad and Naik [18] developed a new quasi 3-D model for the accurate prediction of transverse shear stresses in the laminated composites and sandwiched plates. Plucinski and Jaskowiech [19] presented three-dimensional analysis of laminated plate subjected to mechanical load using two-dimensional numerical model. A detailed review of such higher-order theories and solutions is presented by Sayyad and Ghugal [20-22].

Because of the various applications of composite materials in the field of aerospace engineering where the material is subjected to thermal and hygrothermal stresses; many researchers have presented various theories for the thermal and hygrothermal stress analysis of the composite laminates. This section of the paper deals with literature related to thermal, thermomechanical and hygrothermal stress analysis of composite plates. Cho et al. [23] presented layer-wise theory for analysis of laminates under thermal loading. Bhaskar et al. [24] presented thermoelastic solutions for composite laminates within the framework of linear uncoupled thermoelasticity. Carrera [25] compared different theories formulated on the basis of the principle of virtual work and the Reissner mixed variational theorem (RMVT). The higher-order theory developed by Rohwer et al. [26] for analysis of laminated plates in thermal environment predicts in-plane stresses accurately when applied to thick plates carrying a mechanical load but gives less accurate predictions for sinusoidal thermal loading. A finite element model was proposed by Robaldo and Carrera [27] for the thermoelastic analysis of anisotropic plates. Kant and Shiyekar [28] developed a complete analytical model for the thermal stress analysis of composite laminates under gradient thermal load. A four-variable

plate theory was developed by Sayyad et al. [29] for the thermoelastic flexural analysis of laminated composite plates. Sayyad et al. [30] presented thermal stress analysis of layered composites using exponential shear deformation theory. Zenkour and Radwan [31] presented a hyperbolic model for the analysis of layered plates under thermal load and resting on elastic foundations. Shahravi et al. [32] presented an analytical approach to study the thermal deflections of simply supported composite plates under sinusoidal thermal load. Evran [33] presented finite element analysis of laminated composite plates under constant temperature load using Taguchi method.

Carrera and Nali [34] presented an advanced finite element formulation for the layered plates carrying mechanical, thermal, electrical and magnetic fields. Ali et al [35] proposed a theory for the thermal and mechanical stress analysis of laminated plates, the proposed theory can be used for thick plates and for any combination of thermal and mechanical loading. Zenkour [36] used unified shear deformation theory for flexural analysis of laminated plates under combined thermal and mechanical load. Kant et al. [37] investigated the thermomechanical response of laminated composites using semi-analytical model. Nali and Carrera [38] studied buckling of composite plates under combined thermomechanical load. Wu et al. [39] presented a refined higher-order theory for angle-ply composite laminate subjected to thermomechanical loads. Ghugal and Kulkarni [40, 41] presented a refined sinusoidal theory for thermomechanical stress analysis of cross-ply laminates. Zenkour et al. [42] used unified theory for investigation of bending of cross-ply laminated plates under thermomechanical loads. Wu and Xiaohui [43] presented thermomechanical analysis of multi-layered plates using Reddy-type plate theory considering the effect of transverse normal strain.

Patel et al. [44] studied characteristics of thick composite laminated plates under hygrothermal load using a higher-order theory. Zenkour [45] has investigated the static response of angle-ply laminated plates for variation in temperature and moisture concentrations. A higher-order global-local model is proposed by Wu and Lo [46] for the hygrothermomechanical analysis of laminated composite plates. Najafi et al. [47, 48] studied the environmental effects on mechanical properties of glass/epoxy and fiber metal laminates through experimental investigations because of hygrothermal and isothermal aging. Akbas [49] investigated nonlinear static analysis of composite beams under hygrothermal effects using finite element method. Sayyad and Ghugal [50] presented a

simple four variable shear deformation theory for the bending of functionally graded plates subjected to nonlinear hygrothermomechanical loading. A refined quasi-3D model considering the effect of transverse normal strain and shear deformation for the buckling response of functionally graded plates on elastic foundations under hygrothermomechanical loading is proposed by Zenkour and Radwan [51]. Garg and Chalak [52] presented a critical review of literature related to the behavior of laminated composites and sandwich structures subjected to hygrothermal loading. Moleiro et al. [53] developed an exact 3D hygrothermal elasticity solution for simply supported rectangular composite plates. Das and Niyogi [54] studied free vibrations of epoxy-based cross ply laminated plates subjected to hygrothermal loading. Recently Naik and Sayyad [55] presented an analysis of laminated plates subjected to mechanical and hygrothermal loads using fifth-order shear and normal deformation theory.

In this paper the fifth order shear and normal deformation theory is applied for the cylindrical bending of laminated composite and sandwich plates under thermal and hygrothermal loads. The present theory is developed by Naik and Sayyad [56-58] for laminated and sandwich plates and by Ghumare and Sayyad [59-61] for the analysis of functionally graded plates subjected to mechanical and thermal loads.

Following points summarizes the features of the present study.

1. The main motivation behind the present theory is the contribution and recommendations given by Ali et al. [35], Bhaskar et al. [24] and Erasmo Carrera [62] regarding the stretching of the thickness of the laminated composite plates. Carrera [62] studied the effect of the normal strain on the analysis of homogeneous and layered plates under thermal load and recommended the consideration of the thickness stretching effect for thermal stress analysis of plates particularly when the temperature and moisture concentration varies through the thickness of the plate. Carrera has also recommended to expand the thickness coordinate up to fifth or seventh order for the accurate prediction of the behavior of laminated and sandwich plates under hygrothermomechanical load. Therefore, in the present investigation fifth order shear and normal deformation theory (FOSNDT) is developed for the cylindrical bending of laminated composite and sandwich plates subjected to thermal and hygrothermal loading.

2. Sufficient literature is available on the bi-directional bending of layered plates under thermal loading, while limited literature is

available on the hygrothermal stress analysis of composite plates. Based on the above fact, in the present investigation cylindrical bending of laminated composite plates under thermal and hygrothermal loading is presented.

3. In the present study hygrothermal cylindrical flexural analysis of laminated and sandwich plates is presented for the first time considering the effects of thickness stretching.

4. In the present study, the detailed numerical results and through the thickness distributions of stresses are presented for cylindrical bending of layered and sandwiched plates which will help the researchers to compare and validate their studies.

Following are the some of the advantages of the present theory over the other higher order theories; which can be summarized as below

- The present theory is computationally simple as compared to other non-polynomial theories as it uses polynomial shape function.
- In the well-known theory of Reddy [63], the thickness co-ordinate is expanded up to third-order and it ignores the effect of thickness stretching, while the present theory the thickness co-ordinates are expanded up to fifth order and hence the present theory improves the accuracy.

2. Plate Geometry

In the present study, a rectangular plate of orthotropic fibrous composite is considered. The plate is having length ' a ' along x -direction and ' b ' along the y -direction. The thickness of the plate ' h ' is measured in z -direction. The dimension $b \gg a$, and hence the plate is subjected to cylindrical bending. For the plate under consideration, since the dimension of the plate along the y -direction is assumed to be very long as compared to other dimensions in x - and z -directions, the strain in the y -direction is neglected. The plate is subjected to an out of plane mechanical load $q(x)$, which is acting on the top surface of the plate located at $z = -h/2$ and sinusoidal thermal and hygroscopic load on the top surface. Fig. 1 shows the plate under consideration and the geometry of the plate.

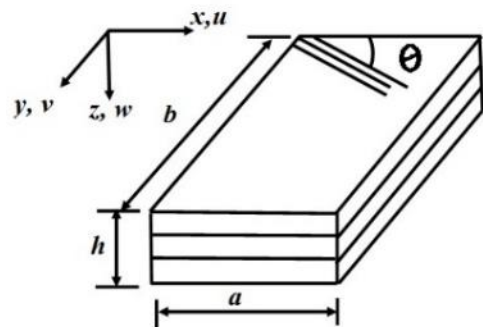


Fig. 1. Plate under consideration and coordinate system

3. Mathematical Formulation

3.1. Displacement field

Following are the assumptions made in the development of the present theory.

- 1) The present theory is displacement-based shear deformation theory
- 2) The in-plane displacements (u) includes three components viz. extension, bending and shear.
- 3) The transverse displacement (w) considers the effect of shear and thickness stretching.
- 4) Three-dimensional Hooke's law is used to determine stresses.

In the present work, the in-plane displacement ' u ' and the transverse displacement ' w ', are considered in polynomial form to accommodate the effect of transverse shear and thickness stretch. The effect of transverse deformation is considered through polynomial shape function expanded up to fifth order in terms of the thickness coordinate. While the derivative of shape function is used in the transverse displacement to accommodate the effect of thickness stretching. There are six variables and the displacement field satisfy the traction free boundaries at the top and bottom surfaces of the plate. The assumed displacement field of the present theory is written as

$$\begin{aligned}
 u(x, z) &= u_0(x) - z \partial w_0 / \partial x \\
 &+ [z - 4z^3 / 3h^2] \phi_x(x) + [z - 16z^5 / 5h^4] \psi_x(x) \\
 w(x, z) &= w_0(x) + (1 - 4z^2 / h^2) \phi_z(x) \\
 &+ (1 - 16z^4 / h^4) \psi_z(x)
 \end{aligned} \tag{1}$$

where ' u ' in in-plane displacement at any point on the plate in x -direction and ' w ' is the displacements in z -direction. ' u_0 ' and ' w_0 ' are the in-plane displacements of mid-plane in x and z -directions respectively. ϕ_x and ψ_x are the rotations about y -axis to account the effect of transverse shear deformation. ϕ_z and ψ_z represent higher-order transverse cross-sectional deformation modes which account the effect of thickness stretching. Eq. (2) shows the non-zero strain components in the present displacement field.

$$\begin{aligned}
 \epsilon_x &= \partial u / \partial x = \partial u_0 / \partial x - z \partial^2 w_0 / \partial x^2 \\
 &+ (z - 4z^3 / 3h^2) \partial \phi_x / \partial x + (z - 16z^5 / 5h^4) \partial \psi_x / \partial x \\
 \epsilon_z &= \partial w / \partial z = (-8z / h^2) \phi_z + (-64z^3 / h^4) \psi_z \\
 \gamma_{xz} &= \partial u / \partial z + \partial w / \partial x = (\phi_x + \partial \phi_z / \partial x)(1 - 4z^2 / h^2) \\
 &+ (\psi_x + \partial \psi_z / \partial x)(1 - 16z^4 / h^4)
 \end{aligned} \tag{2}$$

3.2. Constitutive equations

The co-ordinate system (x - y - z) is used to express the stress-strain relationship. For the k^{th}

lamina the stresses and the strain are related through the relationship given in Eq. (3).

$$\begin{Bmatrix} \sigma_x \\ \sigma_z \\ \tau_{xz} \end{Bmatrix}^k = \begin{bmatrix} Q_{11} & Q_{13} & 0 \\ Q_{13} & Q_{33} & 0 \\ 0 & 0 & Q_{55} \end{bmatrix}^k \begin{Bmatrix} \epsilon_x - \alpha_x \Delta T - \beta_x \Delta C \\ \epsilon_z - \alpha_z \Delta T - \beta_z \Delta C \\ \gamma_{xz} \end{Bmatrix}^k \tag{3}$$

where Q_{11} , Q_{13} , Q_{33} and Q_{55} are the reduced elastic constants in x - z plane and σ_x is the in-plane stress acting along x -direction, σ_z is the stress acting along z -direction and τ_{xz} is the transverse shear stress acting along the z -direction. ϵ_x and ϵ_z are the in-plane and normal strains along x and z -directions respectively, α_x, α_z and β_x, β_z are the coefficients of linear thermal and moisture expansion in x and z -directions respectively. The below mentioned Eq. (4) states the relationship between elastic constants and engineering constants.

$$\begin{aligned}
 Q_{11} &= \frac{E_1(1 - \mu_{23}\mu_{32})}{(1 - \mu_{12}\mu_{21} - \mu_{23}\mu_{32} - \mu_{31}\mu_{13} - 2\mu_{12}\mu_{23}\mu_{31})}, \\
 Q_{13} &= \frac{E_1(\mu_{31} + \mu_{21}\mu_{32})}{(1 - \mu_{12}\mu_{21} - \mu_{23}\mu_{32} - \mu_{31}\mu_{13} - 2\mu_{12}\mu_{23}\mu_{31})}, \\
 Q_{33} &= \frac{E_3(1 - \mu_{12}\mu_{21})}{(1 - \mu_{12}\mu_{21} - \mu_{23}\mu_{32} - \mu_{31}\mu_{13} - 2\mu_{12}\mu_{23}\mu_{31})}, \\
 Q_{55} &= G_{13}Q
 \end{aligned} \tag{4}$$

here E_1 and E_3 are the moduli of elasticity, G_{13} is the modulus of shear and $\mu_{12}, \mu_{21}, \mu_{13}, \mu_{31}, \mu_{23}, \mu_{32}$ are Poisson's ratios; the subscripts 1, 2, 3 correspond to the coordinate system of fibers, while x, y, z directions represent the coordinate systems for the plate. In the present study, the laminated and sandwich plates are analysed for thermal, mechanical and hygrothermal loading. The variations of thermal and moisture load are assumed along the thickness of the plate and are given in Eq. (5).

$$\begin{aligned}
 \Delta T &= T_0 + \frac{z}{h} T_1 + \frac{f_1(z)}{h} T_2 + \frac{f_2(z)}{h} T_3, \\
 \Delta C &= C_0 + \frac{z}{h} C_1 + \frac{f_1(z)}{h} C_2 + \frac{f_2(z)}{h} C_3
 \end{aligned} \tag{5}$$

where, T_0, T_1, T_2 and T_3 are thermal loads, C_0, C_1, C_2 and C_3 are the moisture concentrations.

3.3. Governing equations and boundary conditions

The variationally consistent governing equations and the boundary conditions corresponding to them are derived using the principle of virtual work given in Eq. (6)

$$\begin{aligned}
 &b \int_{-h/2}^{L+h/2} \int_0^L (\sigma_x \delta \epsilon_x + \sigma_z \delta \epsilon_z + \tau_{xz} \delta \gamma_{xz}) dz dx \\
 &- \int_0^L q(x) \delta w dx = 0
 \end{aligned} \tag{6}$$

Integrating Eq. (6) by parts and equating the coefficients of $\delta u_0, \delta w_0, \delta \phi_x, \delta \psi_x, \delta \phi_z$ and $\delta \psi_z$ to zero, six governing equations can be obtained. The Eq. (7) below gives governing equations in terms of stress resultants.

$$\begin{aligned} \delta u_0 &: \partial N_x / \partial x, \\ \delta w_0 &: \partial^2 M_x^b / \partial x^2 + q, \\ \delta \phi_x &: \partial M_x^{S_1} / \partial x - Q_{xz}^1, \\ \delta \psi_x &: \partial M_x^{S_2} / \partial x - Q_{xz}^2, \\ \delta \phi_z &: \partial Q_{xz}^1 / \partial x - Q_z^{S_1}, \\ \delta \psi_z &: \partial Q_{xz}^2 / \partial x - Q_z^{S_2} \end{aligned} \tag{7}$$

The boundary conditions along edges ($x=0, x=a$) are stated in Eq. (8).

$$\begin{aligned} N_x &= 0 \text{ or } u_0 = 0; \\ M_x^b &= 0 \text{ or } dw_0 / dx = 0; \\ dM_x^b / dx &= 0 \text{ or } w_0 = 0; \\ M_x^{S_1} &= 0 \text{ or } \phi_x = 0; \\ M_x^{S_2} &= 0 \text{ or } \psi_x = 0; \\ Q_{xz}^1 &= 0 \text{ or } \phi_z = 0; \\ Q_{xz}^2 &= 0 \text{ or } \psi_z = 0 \end{aligned} \tag{8}$$

In the above governing equations N_x is the in-plane force resultant; M_x^b is the moment resultant; $M_x^{S_1}, M_x^{S_2}$ are the shear moment resultant; Q_{xz}^1 and Q_{xz}^2 ; $Q_z^{S_1}$ and $Q_z^{S_2}$ are the transverse shear and transverse normal stress resultants. Eq. (9) below gives the expressions for all above stress resultants used in the governing equation.

$$\begin{aligned} (N_x, M_x^b, M_x^{S_1}, M_x^{S_2}) &= \int_{-h/2}^{h/2} [1, z, f_1(z), f_2(z)] \sigma_x dz, \\ (Q_{xz}^1, Q_{xz}^2) &= \int_{-h/2}^{h/2} [f_1'(z), f_2'(z)] \tau_{xz} dz, \\ (Q_z^{S_1}, Q_z^{S_2}) &= \int_{-h/2}^{h/2} [f_1''(z), f_2''(z)] \sigma_z dz \end{aligned} \tag{9}$$

Governing equations in terms of unknown variables $\delta u_0, \delta w_0, \delta \phi_x, \delta \psi_x, \delta \phi_z$ and $\delta \psi_z$ can be developed using the expressions of stress resultants. These governing equations along with the mechanical, thermal and moisture coefficients are mentioned in Appendix A.

4. Analytical Solutions

To obtain the analytical solutions of the governing equations for the plates under considerations Navier's solution is used. It is well known that this solution is applicable for simply supported boundary conditions only. For other boundary conditions, numerical methods such as FEM, FDM, GDQ, Meshfree method and other methods can be used.

In the present study, the plates under consideration are carrying a sinusoidally

distributed mechanical and environmental loads on the top surface, whereas the thermal and moisture load are varying linearly across the thickness of the plates. Following are the kinematic boundary conditions.

$$w_0 = 0, N_x = 0, M_x^b = 0, M_x^{S_1} = 0, M_x^{S_2} = 0 \tag{10}$$

For the unknown displacements to be determined and to satisfy the above-mentioned boundary conditions following form of closed form solution is used.

$$\begin{aligned} (u_0, \phi_x, \psi_x) &= \sum_{m=1}^{\infty} (u_m, \phi_{xm}, \psi_{xm}) \cos\left(\frac{m\pi x}{a}\right), \\ (w_0, \phi_z, \psi_z) &= \sum_{m=1}^{\infty} (w_m, \phi_{zm}, \psi_{zm}) \sin\left(\frac{m\pi x}{a}\right) \end{aligned} \tag{11}$$

In the above equation $u_{mn}, w_{mn}, \phi_{xmn}, \psi_{xmn}, \phi_{zmn}$ and ψ_{zmn} are the unknowns to be determined. The mechanical, thermal and moisture loadings are also expressed using double trigonometric Fourier series as stated in Eq. (12).

$$\begin{aligned} q(x) &= \sum_{m=1}^{\infty} q_m \sin\left(\frac{m\pi x}{a}\right), \\ (T_0, T_1, T_2, T_3) &= \sum_{m=1,3,5}^{\infty} (T_{0mn}, T_{1mn}, T_{2mn}, T_{3mn}) \sin\left(\frac{m\pi x}{a}\right), \\ (C_0, C_1, C_2, C_3) &= \sum_{m=1,3,5}^{\infty} (C_{0mn}, C_{1mn}, C_{2mn}, C_{3mn}) \sin\left(\frac{m\pi x}{a}\right) \end{aligned} \tag{12}$$

In the Eq. (12), T_0 and T_1 represent constant and linear temperature profiles respectively, while T_2 and T_3 represent the non-linear temperature profiles. Similarly, C_0 represents constant moisture load, C_1 represents the linear moisture profile, C_2 and C_3 represent the non-linear moisture profile. For the sinusoidally distributed loads, positive integers m and n are taken as unity. Substitution of Eqs. (11) and (12) in governing equation gives a set of equations which are expressed in matrix form as given in Eq. (13) below.

$$\begin{bmatrix} K_{11} & K_{12} & K_{13} & K_{14} & K_{15} & K_{16} \\ & K_{22} & K_{23} & K_{24} & K_{25} & K_{26} \\ & & K_{33} & K_{34} & K_{35} & K_{36} \\ & & & K_{44} & K_{45} & K_{46} \\ \text{symmetric} & & & & K_{55} & K_{56} \\ & & & & & K_{66} \end{bmatrix} \begin{Bmatrix} u_m \\ w_m \\ \phi_{xm} \\ \psi_{xm} \\ \phi_{zm} \\ \psi_{zm} \end{Bmatrix} = \begin{Bmatrix} f_{11} \\ f_{22} \\ f_{33} \\ f_{44} \\ f_{55} \\ f_{66} \end{Bmatrix} \tag{13}$$

The stiffness coefficients $[K_{ij}]$ and the force vectors used in the Eq. (13) are given in the appendix A.

Values of the unknowns i.e. $u_{mn}, w_{mn}, \phi_{xmn}, \psi_{xmn}, \phi_{zmn}$ and ψ_{zmn} obtained from the solution of Eq. (13) are further used to determine the unknown displacements $u_0, w_0, \phi_x, \psi_x, \phi_z$ and ψ_z from the Eq. (11). After

knowing the values of all the unknown variables, one can determine all the displacements and stresses for the plate under consideration using Eqs. (1) - (4).

Transverse shear stress is calculated using equilibrium equation. If the constitutive equation is used to calculate the transverse shear stress, it results in discontinuity at the layer interface, hence to have a single value of transverse shear stress at the layer interface and to avoid discontinuity at the layer interface, transverse shear stress τ_{xz} is calculated using equilibrium equation of theory of elasticity. Because at the layer interface, there must be the same stress in the upper and the lower layer, and this condition is satisfied using equilibrium equation. Eq. (14) states the equilibrium equation used to calculate the transverse shear stress.

$$\tau_{xz}^k = - \int_{h_k}^{h_{k+1}} \frac{\partial \sigma_x^k}{\partial x} dz + C \quad (14)$$

In addition to continuity of the transverse shear stress, this theory also satisfies the continuity condition for in-plane displacement and transverse displacement as stated in Eq. (15).

$$\left\{ \begin{matrix} \bar{u} \\ \bar{w} \end{matrix} \right\}_{\text{layer}=k, \text{interface}=k+1} = \left\{ \begin{matrix} \bar{u} \\ \bar{w} \end{matrix} \right\}_{\text{layer}=k+1, \text{interface}=k+1} \quad (15)$$

5. Solved Numerical Problems

This section deals with the numerical results corresponding to the thermal, hygrothermal and mechanical stress analysis of laminated composite and sandwich plates. The results are presented in Tables 1-6 and graphically plotted in Figs. 2-18. Solutions of the following problems are presented in the present study.

Problem 1: Thermal stress analysis of three-layered (0°/90°/0°) laminated plate.

Problem 2: Stress analysis of three-layered (0°/core/0°) sandwiched sandwich plate under mechanical loading.

Problem 3: Thermal stress analysis of three-layered (0°/core/0°) sandwiched plate.

Problem 4: Hygrothermal stress analysis of two-layered (0°/90°) laminated plate.

Problem 5: Hygrothermal stress analysis of three-layered (0°/90°/0°) laminated plate.

Problem 6: Hygrothermal stress analysis of three-layered (0°/core/0°) sandwiched plate.

Following material properties and non-dimensional forms are used in the present study and the effect of temperature and moisture is considered through the strain and in-plane forces due to temperature and moisture.

Problem 1:

Material properties [24]

$$\begin{aligned} E_1/E_2 = 25, G_{13}/E_3 = 0.5, G_{33}/E_3 = 0.2, \\ \mu_{13} = \mu_{33} = 0.25, \alpha_3/\alpha_1 = 1125 \end{aligned} \quad (16)$$

Non-dimensional forms

$$\begin{aligned} \text{Aspect Ratio } (S) = \frac{a}{h}, \bar{w} = \frac{w}{h\alpha_1 T_0 S^2}, \\ \bar{u} = \frac{u}{h\alpha_1 T_0 S}, (\bar{\sigma}_x, \bar{\tau}_{xz}) = \frac{(\sigma_x, \tau_{xz})}{E_3 \alpha_0 T_0} \end{aligned} \quad (17)$$

Problem 2:

Material properties

Skin material [64]

$$\begin{aligned} E_1 = 131.1 \text{ GPa}, E_2 = E_3 = 6.9 \text{ GPa}, \\ G_{12} = G_{13} = 3.588 \text{ GPa}, G_{23} = 3.088 \text{ GPa}, \\ \mu_{12} = \mu_{13} = 0.32, \mu_{23} = 0.49 \end{aligned}$$

Core Material [65]

$$\begin{aligned} E_1 = 0.2208 \text{ MPa}, E_2 = 0.2001 \text{ MPa}, \\ E_3 = 2760 \text{ MPa}, G_{12} = 16.56 \text{ MPa}, \\ G_{23} = 455.4 \text{ MPa}, G_{31} = 545.1 \text{ MPa}, \\ \mu_{12} = 0.99, \mu_{13} = \mu_{23} = 0.00003 \end{aligned} \quad (18)$$

Non-dimensional forms

$$\begin{aligned} \bar{u} \left(0, -\frac{h}{2} \right) = \frac{bE_3 u}{q_0 h}, \bar{w} \left(\frac{a}{2}, 0 \right) = \frac{100E_3 w h^3 b}{q_0 a^4}, \\ \bar{\sigma}_x \left(\frac{a}{2}, -\frac{h}{2} \right) = \frac{b\sigma_x}{q_0}, \bar{\tau}_{xz} (0, 0) = \frac{b\tau_{xz}}{q_0} \end{aligned} \quad (19)$$

Problem 3:

Material properties

Face Sheet

$$\begin{aligned} E_1 = 172.4 \text{ GPa}, E_2 = 6.89 \text{ GPa}, \\ E_3 = 6.89 \text{ GPa}, \mu_{12} = \mu_{13} = \mu_{23} = 0.25, \\ G_{12} = G_{13} = 3.45 \text{ GPa}, G_{23} = 1.378 \text{ GPa}, \\ \alpha_1 = \alpha_3 = 0.1 \times 10^{-5} \text{ k}^{-1}, \alpha_2 = 2.0 \times 10^{-5} \text{ k}^{-1} \end{aligned}$$

Core

$$\begin{aligned} E_1 = E_2 = 0.276 \text{ GPa}, E_3 = 3.450 \text{ GPa}, \\ \mu_{12} = \mu_{31} = \mu_{32} = 0.25, G_{12} = 0.1104 \text{ GPa}, \\ G_{13} = G_{23} = 0.414 \text{ GPa}, \\ \alpha_1 = \alpha_3 = 0.1 \times 10^{-6} \text{ k}^{-1}, \alpha_2 = 0.2 \times 10^{-5} \text{ k}^{-1} \end{aligned} \quad (20)$$

Non-dimensional forms

$$\begin{aligned} S = \frac{a}{h}, \bar{u} = \frac{u}{S\alpha_1 T_0}, \bar{w} = \frac{h^3 w}{\alpha_1 T_0 a^4}, \\ \bar{\sigma}_x = \frac{\sigma_x}{E_2 \alpha_1 T_0 S^2}, \bar{\tau}_{xz} = \frac{\tau_{xz}}{E_2 \alpha_1 T_0 S} \end{aligned} \quad (21)$$

Problem 4 and 5:

Material properties

$$\begin{aligned} E_1/E_2 = 25, G_{12}/E_2 = 0.5, G_{22}/E_2 = 0.2, \\ \mu_{12} = \mu_{13} = \mu_{23} = \mu_{32} = 0.25, \alpha_2/\alpha_1 = 3, \\ \alpha_1 = 10^{-6} (1/^\circ C), \beta_x = 0, \\ \beta_y = \beta_z = 0.44 (\text{wt \% } H_2O) \end{aligned} \quad (22)$$

Non-dimensional forms

$$\begin{aligned} \bar{u} &= \frac{u(0, b/2, z)h}{\alpha_1 T_0 a}, \bar{v} = \frac{v(0, b/2, z)h}{\alpha_1 T_0 a}, \\ \bar{w} &= \frac{10w(0, 0, z)h}{\alpha_1 T_0 a^2}, \bar{\sigma}_x = \frac{\sigma_x(a/2, b/2, z)}{E_2 \alpha_1 T_0}, \\ \bar{\sigma}_y &= \frac{\sigma_y(a/2, b/2, z)}{E_2 \alpha_1 T_0}, \bar{\tau}_{xy} = \frac{\tau_{xy}(0, 0, z)}{E_2 \alpha_1 T_0}, \\ \bar{\tau}_{xz} &= \frac{\tau_{xz}(0, b/2, z)}{E_2 \alpha_1 T_0}, \bar{\tau}_{yz} = \frac{\tau_{yz}(a/2, 0, z)}{E_2 \alpha_1 T_0} \end{aligned} \tag{23}$$

In the material properties mentioned above, 1, 2 and 3 refer to directions parallel and perpendicular to the fibers respectively.

Problem 6

Carbon fiber reinforced polymer skin material
 $E_1 = 172.4 \text{ GPa}, E_2 = 6.89 \text{ GPa},$
 $E_3 = 6.89 \text{ GPa}, \mu_{12} = \mu_{13} = \mu_{23} = 0.25,$
 $G_{12} = G_{13} = 3.45 \text{ GPa}, G_{23} = 1.378 \text{ GPa},$ (24)
 $\alpha_1 = 0.5 \times 10^{-6} / ^\circ\text{K}, \alpha_2 = \alpha_3 = 35 \times 10^{-6} / ^\circ\text{K},$
 $\beta_1 = 0, \beta_2 = \beta_3 = 0.004 \text{ wt \% H}_2\text{O}$

PVC foam core material

$E_1 = E_2 = 0.276 \text{ GPa}, E_3 = 3.450 \text{ GPa},$
 $\mu_{12} = \mu_{31} = \mu_{32} = 0.25, G_{12} = 0.1104 \text{ GPa},$
 $G_{13} = G_{23} = 0.414 \text{ GPa},$ (25)
 $\alpha_1 = \alpha_2 = \alpha_3 = 40 \times 10^{-6} / ^\circ\text{K},$
 $\beta_1 = \beta_2 = \beta_3 = 0.003 \text{ wt \% H}_2\text{O}$

Non-dimensional forms

$$\begin{aligned} \bar{u} &= \frac{u(0, b/2, z)h}{\alpha_1 T_0 a}, \bar{v} = \frac{v(0, b/2, z)h}{\alpha_1 T_0 a}, \\ \bar{w} &= \frac{100w(0, 0, z)h}{\alpha_1 T_0 a^2}, \bar{\sigma}_x = \frac{\sigma_x(a/2, b/2, z)}{E_2 \alpha_1 T_0}, \\ \bar{\sigma}_y &= \frac{\sigma_y(a/2, b/2, z)}{E_2 \alpha_1 T_0}, \bar{\tau}_{xy} = \frac{\tau_{xy}(0, 0, z)}{E_2 \alpha_1 T_0}, \\ \bar{\tau}_{xz} &= \frac{\tau_{xz}(0, b/2, z)}{E_2 \alpha_1 T_0}, \bar{\tau}_{yz} = \frac{\tau_{yz}(a/2, 0, z)}{E_2 \alpha_1 T_0} \end{aligned} \tag{26}$$

6. Results and Discussion

Problem 1: In this problem bending of a (0°/90°/0°) laminate plate subjected to sinusoidally distributed thermal load over the surface of the plate and linearly distributed across the thickness of the plate is discussed. The plate is having thickness of each layer as $h/3$. The material properties used for this problem are given in Eq. (16), while Eq. (17) gives non-dimensional forms for the calculations of displacements and stresses. Numerical results obtained are summarized in Table 1 for this problem. The results obtained by the present FOSNDT are compared with the elasticity solution presented by Bhaskar et al. [24]. The comparison of results is done for different aspect ratio ($a/h = 4, 10, 20, 50, 100$). The comparison reveals that the present theory gives results which are close to the elasticity solution.

Variation in transverse displacement with aspect ratio is plotted in Fig. 2, while through-the-thickness variations of displacements and stresses are presented in Figs. 3-5 for $a/h = 4$.

Problem 2: In this problem the present theory before it is application to thermal stress analysis of sandwich plate, it is applied to a sandwich plate subjected to sinusoidal mechanical loading. The top and bottom layers are having thickness $0.1h$, while the thickness of the middle core is $0.8h$. The material properties and the non-dimensional forms used are given in Eqs. (18) and (19). The results obtained using present theory are compared with those predicted by sinusoidal shear and normal plate theory (SSNPT) of Sayyad and Ghugal [66], higher order shear deformation theory (HSST) of Reddy [63], first order shear deformation theory (FSDT) of Mindlin [8] and classical plate theory (CPT) of Kirchhoff [7]. The comparison is shown in Table 2 reveals that the present theory gives results in good agreement with SSNPT and HSST.

Table 1. Comparison of deflections and stresses for (0°/90°/0°) laminated plate under cylindrical bending subjected to the linear temperature field

S	Model	$\bar{u} (\pm h/2)$	% Error	$\bar{w} (\pm h/2)$	% Error	$\bar{\sigma}_x (\pm h/6)$	% Error	$\bar{\tau}_{xz} (\pm h/6)$	% Error
4	Present	7.206	-3.5341	18.55	1.255	375.6	0.886	3.033	7.173
	Bhaskar et al. [24]	7.470	-	18.32	-	372.3	-	2.830	-
10	Present	4.976	-0.6588	5.441	0.610	375.1	0.914	2.441	-5.387
	Bhaskar et al. [24]	5.009	-	5.408	-	371.7	-	2.580	-
20	Present	4.564	-0.5447	3.476	-0.086	375.0	0.942	1.376	-4.510
	Bhaskar et al. [24]	4.589	-	3.479	-	371.5	-	1.441	-
50	Present	4.444	-0.5148	2.920	-0.443	374.9	0.942	0.569	-4.208
	Bhaskar et al. [24]	4.467	-	2.933	-	371.4	-	0.594	-
100	Present	4.426	-0.5169	2.840	-0.525	374.9	0.942	0.286	-4.026
	Bhaskar et al. [24]	4.449	-	2.855	-	371.4	-	0.298	-
	CPT [7]	4.444	-	2.829	-	371.4	-	-	-

For a thin plate having an aspect ratio equal to 100, present theory gives results almost equal to those predicted by the other theories. It shows that the present theory can be applied efficiently to analyse sandwich plates as well.

Problem 3: In this problem bending response of $(0^0/core/0^0)$ sandwich plate subjected to sinusoidal thermal load is studied. For the plate under consideration; the face sheets are having a thickness equal to $0.1h$ and the core is of thickness $0.8h$. The material properties stated in Eq. (20) are used in the present example and the non-dimensional forms stated in Eq. (21) are used for the calculations of unknown displacements and stresses.

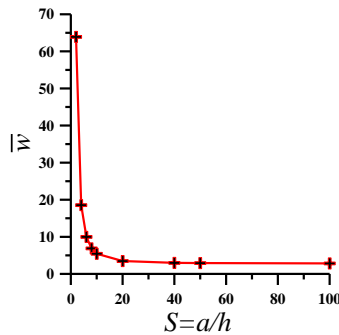


Fig. 2. Variation of non-dimensional transverse displacement (\bar{w}) with respect to the aspect ratio (S) for $(0^0/90^0/0^0)$ laminated plate subjected to linear thermal load

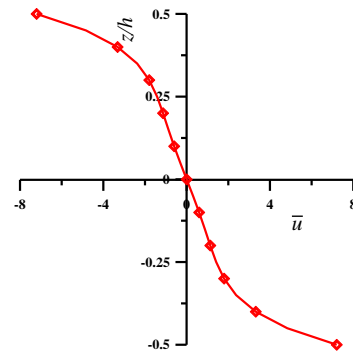


Fig. 3. Variation of non-dimensional in-plane displacement (\bar{u}) along the thickness for $(0^0/90^0/0^0)$ laminated plate subjected to linear thermal load

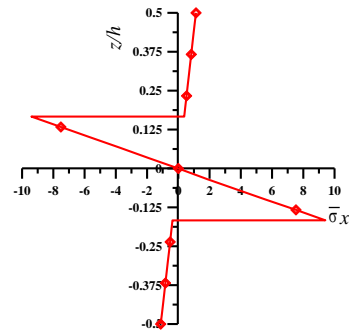


Fig. 4. Variation of non-dimensional in-plane normal stress ($\bar{\sigma}_x$) along the thickness for $(0^0/90^0/0^0)$ laminated plate subjected to linear thermal load

Table 2. Comparison of deflections and stresses for $(0^0/core/0^0)$ sandwich plate under cylindrical bending subjected to sinusoidal mechanical load

a/h	ε_z	Model	$\bar{u} (\pm h/2)$	$\bar{w} (\pm h/2)$	$\bar{\sigma}_x (\pm h/2)$	$\bar{\tau}_{xz} (\pm 0.4h)$
4	$\neq 0$	FOSNDT	1.9096	8.6150	28.8295	1.4005
	$\neq 0$	SSNPT [66]	1.8901	8.4532	28.9670	1.3841
	0	HSDT [63]	1.9081	8.5369	28.6061	1.3855
	0	FSDT [8]	1.3295	5.4694	19.9320	1.4089
	0	CPT [7]	1.3295	1.3225	19.9320	1.4089
10	$\neq 0$	FOSNDT	22.203	2.4914	133.100	3.5242
	$\neq 0$	SSNPT [66]	22.092	2.4739	133.754	3.5122
	0	HSDT [63]	22.235	2.4889	133.340	3.5128
	0	FSDT [8]	20.773	1.9860	124.575	3.5223
	0	CPT [7]	20.773	1.3225	124.575	3.5223
100	$\neq 0$	FOSNDT	20781.0	1.3337	12433.0	35.285
	$\neq 0$	SSNPT [66]	20680.2	1.3272	12477.5	35.220
	0	HSDT [63]	20.788.4	1.3342	12466.4	35.222
	0	FSDT [8]	20773.2	1.3291	12457.3	35.221
	0	CPT [7]	20773.2	1.3225	12457.3	35.221

This problem is presented for the first time in this paper and no results are reported in the literature, hence only present results are tabulated in Table 3. Variation in transverse displacement with respect to aspect ratio is plotted in Fig. 6 and variations of normalized displacements and stresses along the thickness are plotted in Figs. 7-9 for $a/h = 4$. Since in the literature no results are available for this problem, the results presented in this paper will serve as a benchmark solution for the future research.

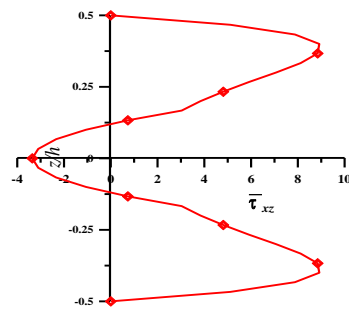


Fig. 5. Variation of non-dimensional transverse shear stress ($\bar{\tau}_{xz}$) along the thickness for $(0^0/90^0/0^0)$ laminated plate subjected to linear thermal load

Table 3. Deflections and stresses in $(0^0/core/0^0)$ sandwich plate subjected to the linear temperature field using present FOSNDT

S	$\bar{u} (\pm h/2)$	$\bar{w} (\pm h/2)$	$\bar{\sigma}_x (\pm h/2)$	$\bar{\tau}_{xz} (\pm 0.4h)$
4	0.0990	20.589	0.0526	0.0075
10	0.0387	2.5890	0.0058	0.0012
20	0.0193	0.6220	0.0017	0.0000
50	0.0077	0.0980	0.0002	0.0000
100	0.0039	0.0250	0.0000	0.0000

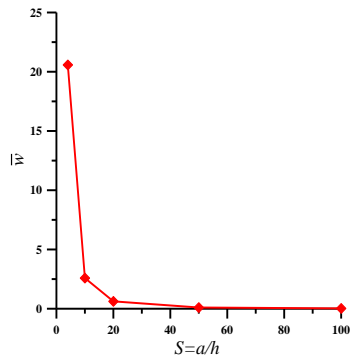


Fig. 6. Variation of non-dimensional transverse displacement (\bar{w}) with respect to aspect ratio (S) for $(0^0/core/0^0)$ sandwich plate subjected to linear thermal load

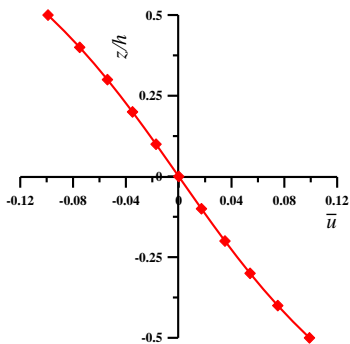


Fig. 7. Variation of non-dimensional in-plane displacement (\bar{u}) along the thickness for $(0^0/core/0^0)$ sandwich plate subjected to linear thermal load

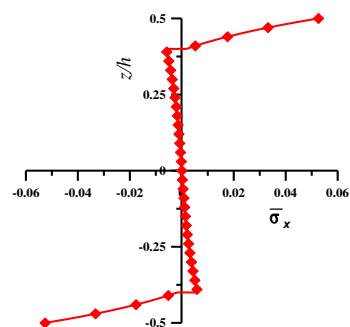


Fig. 8. Variation of non-dimensional in-plane normal stress ($\bar{\sigma}_x$) along the thickness for $(0^0/core/0^0)$ sandwich plate subjected to linear thermal load

Problem 4: In this problem bending of $(0^0/90^0)$ laminated plate subjected to linearly varying hygrothermal load, and having material properties given in Eq. (22) is presented. The non-dimensional forms stated in Eq. (23) are used to calculate the displacement and stresses.

Each layer of the plate is having a thickness equal to $h/2$. Only results obtained using the present theory are summarized in this paper in Table 4 and the same are plotted for $a/h = 4$ in Figs. 10- 12.

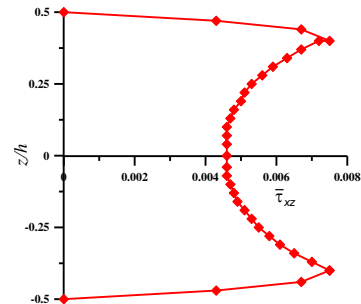


Fig. 9. Variation of non-dimensional transverse shear stress ($\bar{\tau}_{xz}$) along the thickness for $(0^0/core/0^0)$ sandwich plate subjected to linear thermal load

Table 4. Deflections and stresses in $(0^0/90^0)$ laminated plate subjected to the linear hygrothermal loading for present FOSNDT ($T_0=100.0$; $T_{0M}=0$; $T_{1M}=T_0$; $T_{2M}=0$; $T_{3M}=0$; $C_0=3 \times 10^{-4}$; $C_{0M}=0$; $C_{1M}=C_0$; $C_{2M}=0$; $C_{3M}=0$)

S	$\bar{u} (-h/2)$	$\bar{w} (-h/2)$	$\bar{\sigma}_x (-h/2)$	$\bar{\tau}_{xz} (0)$
4	0.0482	1.6432	2.2784	-0.1326
10	0.0191	1.4783	2.1355	-0.0529
20	0.0096	1.4539	2.1433	-0.0265
50	0.0038	1.4470	2.1480	-0.0106
100	0.0019	1.4460	2.1488	-0.0053

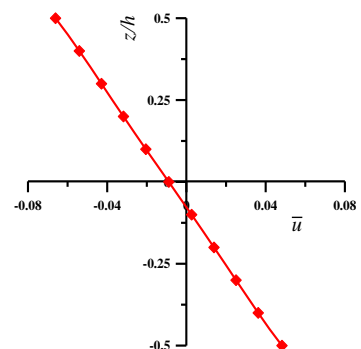


Fig. 10. Variation of non-dimensional in-plane displacement (\bar{u}) along the thickness for $(0^0/90^0)$ laminated plate subjected to linear hygrothermal load

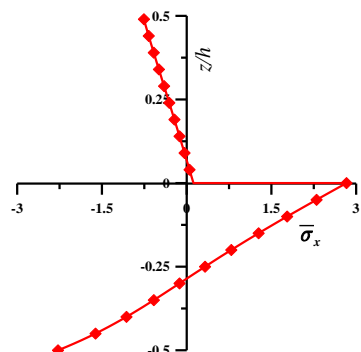


Fig. 11. Variation of non-dimensional in-plane normal stress ($\bar{\sigma}_x$) along the thickness for $(0^0/90^0)$ laminated plate subjected to linear hygrothermal load

Problem 5: In this problem bending of $(0^0/90^0/0^0)$ laminated plate subjected to linearly varying hygrothermal load is presented. All the layers are having equal thickness i.e., $h/3$ and having the material properties stated in Eq. (22). The non-dimensional forms mentioned in the Eq. (23) are used to obtain results. The results obtained using the present theory are tabulated in Table 5 and plotted in Figs. 13-15.

Problem 6: A sandwich plate $(0^0/core/0^0)$ subjected to linearly varying hygrothermal load is analyzed in this problem. Thickness of each face sheet is assumed as $0.1h$ and core is having a thickness of $0.8h$, where h is the thickness of the plate under consideration.

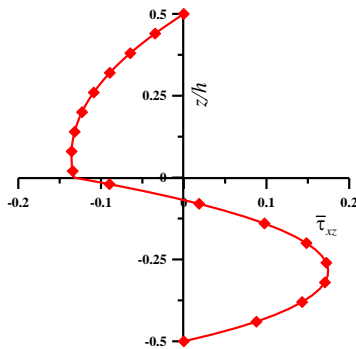


Fig. 12. Variation of non-dimensional transverse shear stress ($\bar{\tau}_{xz}$) along the thickness for $(0^0/core/0^0)$ sandwich plate subjected to linear thermal load

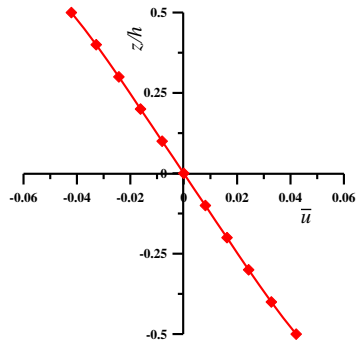


Fig. 13. Variation of non-dimensional in-plane displacement (\bar{u}) along the thickness for $(0^0/90^0/0^0)$ laminated plate subjected to linear hygrothermal load

Table 5. Deflections and stresses in $(0^0/90^0/0^0)$ laminated plate subjected to the linear hygrothermal loading for present FOSNDT ($T_0=100.0$; $T_{0M}=0$; $T_{1M}=T_0$; $T_{2M}=0$; $T_{3M}=0$; $C_0=3 \times 10^{-4}$; $C_{0M}=0$; $C_{1M}=C_0$; $C_{2M}=0$; $C_{3M}=0$)

S	$\bar{u}(-h/2)$	$\bar{w}(-h/2)$	$\bar{\sigma}_x(-h/2)$	$\bar{\tau}_{xz}(0)$
4	0.0421	1.2590	-0.3504	-0.0237
10	0.0165	1.0824	-0.1013	-0.0075
20	0.0082	1.0558	-0.0556	-0.0035
50	0.0033	1.0483	-0.0423	-0.0014
100	0.0016	1.0473	-0.0403	0.0000

The plate is having a skin of orthotropic carbon fiber reinforced polymer (CFRP) and the core is made of polyvinyl chloride (PVC). The face sheet is having material properties as given in Eq. (24) while those used for the core are given in Eq. (25). The non-dimensional displacements and stresses are calculated using the non-dimensional forms stated in Eq. (26). The results are presented in Table 6 and are plotted in Figs. 16-18. Only the results obtained using present FOSNDT are given in the table as no results are available in the literature for the cylindrical bending of sandwich plates subjected to hygrothermal loading.

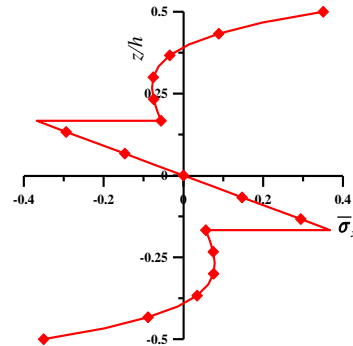


Fig. 14. Variation of non-dimensional in-plane normal stress ($\bar{\sigma}_x$) along the thickness for $(0^0/90^0/0^0)$ laminated plate subjected to linear hygrothermal load

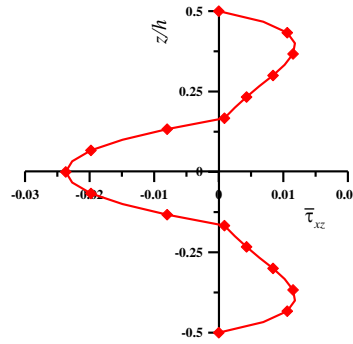


Fig. 15. Variation of non-dimensional transverse shear stress ($\bar{\tau}_{xz}$) along the thickness for $(0^0/90^0/0^0)$ laminated plate subjected to linear hygrothermal load

Table 6 Deflections and stresses in $(0^0/core/0^0)$ sandwich plate subjected to the linear hygrothermal loading for present FOSNDT ($T_0=100.0$; $T_{0M}=0$; $T_{1M}=T_0$; $T_{2M}=0$; $T_{3M}=0$; $C_0=3 \times 10^{-4}$; $C_{0M}=0$; $C_{1M}=C_0$; $C_{2M}=0$; $C_{3M}=0$)

S	$\bar{u}(-h/2)$	$\bar{w}(-h/2)$	$\bar{\sigma}_x(-h/2)$	$\bar{\tau}_{xz}(0)$
4	0.0878	3.9846	-6.4290	-0.0269
10	0.0307	0.2617	-2.9577	-0.0083
20	0.0151	0.0520	-2.4656	-0.0040
50	0.0060	0.0077	-2.3280	-0.0016
100	0.0030	0.0019	-2.3084	0.0000

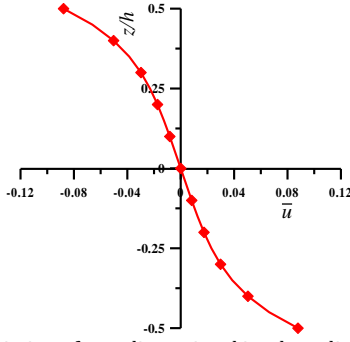


Fig. 16. Variation of non-dimensional in-plane displacement (\bar{u}) along the thickness for $(0^0/core/0^0)$ sandwich plate subjected to linear hygrothermal load

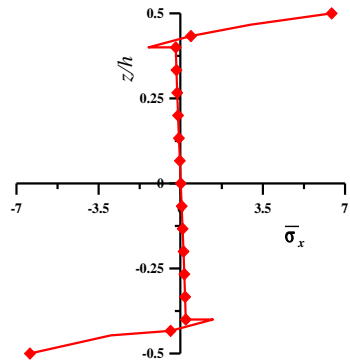


Fig. 17. Variation of non-dimensional in-plane normal stress ($\bar{\sigma}_x$) along the thickness for $(0^0/core/0^0)$ sandwich plate subjected to linear hygrothermal load

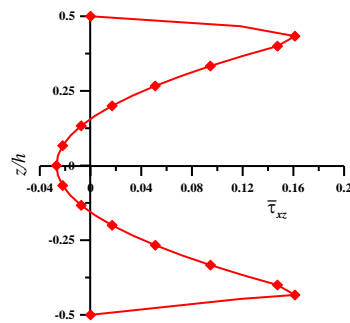


Fig. 18. Variation of non-dimensional transverse shear stress ($\bar{\tau}_{xz}$) along the thickness for $(0^0/core/0^0)$ sandwich plate subjected to linear hygrothermal load

7. Conclusions

This paper presents a new displacement-based fifth-order shear and normal deformation theory (FOSNDT) for the thermal and hygrothermal stress analysis of layered composite and sandwiches having one dimension infinitely long. To assess the performance of the present theory, the results are generated for cylindrical bending of $0^0/90^0/0^0$ plate carrying linear thermal load. The results obtained are compared with the available elasticity solution. The comparison shows that the present theory predicts the in-plane displacement, transverse displacement in close agreement with the elasticity solution. The percentage error in the prediction of in-plane displacement is -3.5341% for aspect ratio 4 and reduces to -0.51% for a

plate having aspect ratio 100. For the transverse displacement and in-plane stress the percentage error in prediction decreases with increase in aspect ratio. Thus, it can be concluded that the present theory under predicts the in-plane displacement and over predicts the transverse displacement and in-plane stresses. The transverse shear stress prediction using the present theory is on the higher side as compared to the elasticity solution. Similarly for the sandwich plate under mechanical loading the present theory predicts the behaviour in good agreement with other well established theories.

For cylindrical bending of layered composites and sandwiches under hygrothermal load results are not reported in the literature for comparison. Hence, in the present paper the results generated for cylindrical bending of laminated and sandwich plates for hygrothermal loading are presented without comparison, but after validating the theory for thermal loading, and mechanical loading thus these results will serve as a benchmark for the future research.

Appendix A

Following are the governing equations derived by applying principle of virtual work in Eq. (6),

$$\begin{aligned} \delta u_0 : \frac{\partial N_x}{\partial x} = & A_{11} \frac{\partial^2 u_0}{\partial x^2} - B_{11} \frac{\partial^3 w_0}{\partial x^3} + C_{11} \frac{\partial^2 \phi_x}{\partial x^2} \\ & + D_{11} \frac{\partial^2 \psi_x}{\partial x^2} + I_{13} \frac{\partial \phi_x}{\partial x} + J_{13} \frac{\partial \psi_x}{\partial x} - \left(A_{11}^T \frac{\partial T_0}{\partial x} \right. \\ & + \frac{B_{11}^T}{h} \frac{\partial T_1}{\partial x} + \frac{C_{11}^T}{h} \frac{\partial T_2}{\partial x} + \frac{D_{11}^T}{h} \frac{\partial T_3}{\partial x} \left. \right) - \left(A_{13}^T \frac{\partial T_0}{\partial x} \right. \\ & + \frac{B_{13}^T}{h} \frac{\partial T_1}{\partial x} + \frac{C_{13}^T}{h} \frac{\partial T_2}{\partial x} + \frac{D_{13}^T}{h} \frac{\partial T_3}{\partial x} \left. \right) - \left(A_{11}^C \frac{\partial C_0}{\partial x} \right. \\ & + \frac{B_{11}^C}{h} \frac{\partial C_1}{\partial x} + \frac{C_{11}^C}{h} \frac{\partial C_2}{\partial x} + \frac{D_{11}^C}{h} \frac{\partial C_3}{\partial x} \left. \right) \\ & - \left(A_{13}^C \frac{\partial C_0}{\partial x} + \frac{B_{13}^C}{h} \frac{\partial C_1}{\partial x} + \frac{C_{13}^C}{h} \frac{\partial C_2}{\partial x} \right. \\ & \left. + \frac{D_{13}^C}{h} \frac{\partial C_3}{\partial x} \right) = 0 \end{aligned} \tag{A.1}$$

$$\begin{aligned} \delta w_0 : \frac{\partial^2 M_x^b}{\partial x^2} + q = & B_{11} \frac{\partial^3 u_0}{\partial x^3} - A_{s11} \frac{\partial^4 w_0}{\partial x^4} \\ & + C_{s11} \frac{\partial^3 \phi_x}{\partial x^3} + D_{s11} \frac{\partial^3 \psi_x}{\partial x^3} + I_{s13} \frac{\partial^2 \phi_x}{\partial x^2} + J_{s13} \frac{\partial^2 \psi_x}{\partial x^2} \\ & - \left(B_{11}^T \frac{\partial^2 T_0}{\partial x^2} + \frac{A_{s11}^T}{h} \frac{\partial^2 T_1}{\partial x^2} + \frac{C_{s11}^T}{h} \frac{\partial^2 T_2}{\partial x^2} \right. \\ & \left. + \frac{D_{s11}^T}{h} \frac{\partial^2 T_3}{\partial x^2} \right) - \left(B_{13}^T \frac{\partial^2 T_0}{\partial x^2} + \frac{A_{s13}^T}{h} \frac{\partial^2 T_1}{\partial x^2} \right. \\ & \left. + \frac{C_{s13}^T}{h} \frac{\partial^2 T_2}{\partial x^2} + \frac{D_{s13}^T}{h} \frac{\partial^2 T_3}{\partial x^2} \right) - \left(B_{11}^C \frac{\partial^2 C_0}{\partial x^2} \right. \\ & \left. + \frac{A_{s11}^C}{h} \frac{\partial^2 C_1}{\partial x^2} + \frac{C_{s11}^C}{h} \frac{\partial^2 C_2}{\partial x^2} + \frac{D_{s11}^C}{h} \frac{\partial^2 C_3}{\partial x^2} \right) \\ & - \left(B_{13}^C \frac{\partial^2 C_0}{\partial x^2} + \frac{A_{s13}^C}{h} \frac{\partial^2 C_1}{\partial x^2} + \frac{C_{s13}^C}{h} \frac{\partial^2 C_2}{\partial x^2} \right. \\ & \left. + \frac{D_{s13}^C}{h} \frac{\partial^2 C_3}{\partial x^2} \right) - q = 0 \end{aligned} \tag{A.2}$$

$$\begin{aligned}
 \delta\phi_x : \frac{\partial M_x^{S_1}}{\partial x} - Q_{xz}^1 = C_{11} \frac{\partial^2 u_0}{\partial x^2} - C_{s11} \frac{\partial^3 w_0}{\partial x^3} \\
 + C_{ss111} \frac{\partial^2 \phi_x}{\partial x^2} + C_{ss211} \frac{\partial^2 \psi_x}{\partial x^2} + I_{ss113} \frac{\partial \phi_z}{\partial x} \\
 + J_{ss113} \frac{\partial \psi_z}{\partial x} - C_{sss155} \phi_x - C_{sss155} \frac{\partial \phi_z}{\partial x} \\
 - C_{sss255} \psi_x - C_{sss255} \frac{\partial \psi_z}{\partial x} - \left(C_{11}^{T_x} \frac{\partial T_0}{\partial x} \right. \\
 \left. + \frac{C_{s11}^{T_x}}{h} \frac{\partial T_1}{\partial x} + \frac{C_{ss111}^{T_x}}{h} \frac{\partial T_2}{\partial x} + \frac{C_{ss211}^{T_x}}{h} \frac{\partial T_3}{\partial x} \right) \\
 - \left(C_{13}^{T_z} \frac{\partial T_0}{\partial x} + \frac{C_{s13}^{T_z}}{h} \frac{\partial T_1}{\partial x} + \frac{C_{ss113}^{T_z}}{h} \frac{\partial T_2}{\partial x} \right. \\
 \left. + \frac{C_{ss213}^{T_z}}{h} \frac{\partial T_3}{\partial x} \right) - \left(C_{11}^{C_x} \frac{\partial C_0}{\partial x} + \frac{C_{s11}^{C_x}}{h} \frac{\partial C_1}{\partial x} \right. \\
 \left. + \frac{C_{ss111}^{C_x}}{h} \frac{\partial C_2}{\partial x} + \frac{C_{ss211}^{C_x}}{h} \frac{\partial C_3}{\partial x} \right) - \left(C_{13}^{C_z} \frac{\partial C_0}{\partial x} \right. \\
 \left. + \frac{C_{s13}^{C_z}}{h} \frac{\partial C_1}{\partial x} + \frac{C_{ss113}^{C_z}}{h} \frac{\partial C_2}{\partial x} + \frac{C_{ss213}^{C_z}}{h} \frac{\partial C_3}{\partial x} \right) = 0 \quad (A.3)
 \end{aligned}$$

$$\begin{aligned}
 \psi_x : \frac{\partial M_x^{S_2}}{\partial x} - Q_{xz}^2 = D_{11} \frac{\partial^2 u_0}{\partial x^2} - D_{s11} \frac{\partial^3 w_0}{\partial x^3} \\
 + C_{ss211} \frac{\partial^2 \phi_x}{\partial x^2} + D_{ss111} \frac{\partial^2 \psi_x}{\partial x^2} + I_{ss213} \frac{\partial \phi_z}{\partial x} \\
 + J_{ss213} \frac{\partial \psi_z}{\partial x} - C_{sss255} \phi_x - C_{sss255} \frac{\partial \phi_z}{\partial x} \\
 - D_{sss155} \psi_x - D_{sss155} \frac{\partial \psi_z}{\partial x} - \left(D_{11}^{T_x} \frac{\partial T_0}{\partial x} \right. \\
 \left. + \frac{D_{s11}^{T_x}}{h} \frac{\partial T_1}{\partial x} + \frac{C_{ss211}^{T_x}}{h} \frac{\partial T_2}{\partial x} + \frac{D_{ss111}^{T_x}}{h} \frac{\partial T_3}{\partial x} \right) \\
 - \left(D_{13}^{T_z} \frac{\partial T_0}{\partial x} + \frac{D_{s13}^{T_z}}{h} \frac{\partial T_1}{\partial x} + \frac{C_{ss213}^{T_z}}{h} \frac{\partial T_2}{\partial x} \right. \\
 \left. + \frac{D_{ss113}^{T_z}}{h} \frac{\partial T_3}{\partial x} \right) - \left(D_{11}^{C_x} \frac{\partial C_0}{\partial x} + \frac{D_{s11}^{C_x}}{h} \frac{\partial C_1}{\partial x} \right. \\
 \left. + \frac{C_{ss211}^{C_x}}{h} \frac{\partial C_2}{\partial x} + \frac{D_{ss111}^{C_x}}{h} \frac{\partial C_3}{\partial x} \right) - \left(D_{13}^{C_z} \frac{\partial C_0}{\partial x} \right. \\
 \left. + \frac{D_{s13}^{C_z}}{h} \frac{\partial C_1}{\partial x} + \frac{C_{ss213}^{C_z}}{h} \frac{\partial C_2}{\partial x} + \frac{D_{ss113}^{C_z}}{h} \frac{\partial C_3}{\partial x} \right) = 0 \quad (A.4)
 \end{aligned}$$

$$\begin{aligned}
 \delta\phi_z : \frac{\partial Q_{xz}^1}{\partial x} - Q_z^{S_1} = C_{sss155} \frac{\partial \phi_x}{\partial x} + C_{sss155} \frac{\partial^2 \phi_z}{\partial x^2} \\
 + C_{sss255} \frac{\partial \psi_x}{\partial x} + C_{sss255} \frac{\partial^2 \psi_z}{\partial x^2} - I_{13} \frac{\partial u_0}{\partial x} \\
 + I_{s13} \frac{\partial^2 w_0}{\partial x^2} - I_{ss113} \frac{\partial \phi_x}{\partial x} - I_{ss213} \frac{\partial \psi_x}{\partial x} - I_{sss133} \phi_z \\
 - I_{sss233} \psi_z + \left(I_{13}^{T_x} T_0 + \frac{I_{s13}^{T_x}}{h} T_1 + \frac{I_{ss113}^{T_x}}{h} T_2 \right. \\
 \left. + \frac{I_{ss213}^{T_x}}{h} T_3 \right) + \left(I_{33}^{T_z} T_0 + \frac{I_{s33}^{T_z}}{h} T_1 + \frac{I_{ss133}^{T_z}}{h} T_2 \right. \\
 \left. + \frac{I_{ss233}^{T_z}}{h} T_3 \right) + \left(I_{13}^{C_x} T_0 + \frac{I_{s13}^{C_x}}{h} C_1 + \frac{I_{ss113}^{C_x}}{h} C_2 \right. \\
 \left. + \frac{I_{ss213}^{C_x}}{h} C_3 \right) + \left(I_{33}^{C_z} C_0 + \frac{I_{s33}^{C_z}}{h} C_1 + \frac{I_{ss133}^{C_z}}{h} C_2 \right. \\
 \left. + \frac{I_{ss233}^{C_z}}{h} C_3 \right) = 0 \quad (A.5)
 \end{aligned}$$

$$\begin{aligned}
 \delta\psi_z : \frac{\partial Q_{xz}^2}{\partial x} - Q_z^{S_2} = C_{sss255} \frac{\partial \phi_x}{\partial x} + C_{sss255} \frac{\partial^2 \phi_z}{\partial x^2} \\
 + D_{sss155} \frac{\partial \psi_x}{\partial x} + D_{sss155} \frac{\partial^2 \psi_z}{\partial x^2} - J_{13} \frac{\partial u_0}{\partial x} \\
 + J_{s13} \frac{\partial^2 w_0}{\partial x^2} - J_{ss113} \frac{\partial \phi_x}{\partial x} - J_{ss213} \frac{\partial \psi_x}{\partial x} - I_{sss233} \phi_z \quad (A.6) \\
 - J_{sss133} \psi_z + \left(J_{13}^{T_x} T_0 + \frac{J_{s13}^{T_x}}{h} T_1 + \frac{J_{ss113}^{T_x}}{h} T_2 \right. \\
 \left. + \frac{J_{ss213}^{T_x}}{h} T_3 \right) + \left(J_{33}^{T_z} T_0 + \frac{J_{s33}^{T_z}}{h} T_1 + \frac{J_{ss133}^{T_z}}{h} T_2 \right. \\
 \left. + \frac{J_{ss233}^{T_z}}{h} T_3 \right) + \left(J_{13}^{C_x} C_0 + \frac{J_{s13}^{C_x}}{h} C_1 + \frac{J_{ss113}^{C_x}}{h} C_2 \right. \\
 \left. + \frac{J_{ss213}^{C_x}}{h} C_3 \right) + \left(J_{33}^{C_z} C_0 + \frac{J_{s33}^{C_z}}{h} C_1 + \frac{J_{ss133}^{C_z}}{h} C_2 \right. \\
 \left. + \frac{J_{ss233}^{C_z}}{h} C_3 \right) = 0
 \end{aligned}$$

Mechanical coefficients

$$\begin{aligned}
 (A_{ij}, B_{ij}, A_{sij}) = Q_{ij} \int_{-h/2}^{+h/2} (1, z, z^2) dz, \\
 (C_{ij}, C_{sij}, C_{ss1ij}, C_{ss2ij}, I_{ss1ij}, J_{ss1ij}) = \\
 Q_{ij} \int_{-h/2}^{+h/2} f_1(z) [1, z, f_1(z), f_2(z), f_1''(z), f_2''(z)] dz, \\
 (D_{ij}, D_{sij}, D_{ss1ij}, I_{ss2ij}, J_{ss2ij}) = \\
 Q_{ij} \int_{-h/2}^{+h/2} f_2(z) [1, z, f_2(z), f_1''(z), f_2''(z)] dz, \\
 (C_{sss1ij}, C_{sss2ij}) = Q_{ij} \int_{-h/2}^{+h/2} f_1'(z) [f_1'(z), f_2'(z)] dz, \\
 (D_{sss1ij}) = Q_{ij} \int_{-h/2}^{+h/2} f_2'(z) f_2'(z) dz, \\
 (I_{ij}, I_{sij}, I_{ss1ij}, I_{ss2ij}) = \\
 Q_{ij} \int_{-h/2}^{+h/2} f_1''(z) [1, z, f_1''(z), f_2''(z)] dz, \\
 (J_{ij}, J_{sij}, J_{ss1ij}) = Q_{ij} \int_{-h/2}^{+h/2} f_2''(z) [1, z, f_2''(z)] dz, \quad (A.7)
 \end{aligned}$$

Thermal Coefficients

$$\begin{aligned}
 (A_{ij}^{T_z}, B_{ij}^{T_z}, A_{sij}^{T_z}) = Q_{ij} \alpha_z \int_{-h/2}^{+h/2} (1, z, z^2) dz, \\
 (C_{ij}^{T_x}, C_{sij}^{T_x}, C_{ss1ij}^{T_x}, C_{ss2ij}^{T_x}, I_{ss1ij}^{T_x}, J_{ss1ij}^{T_x}) = \\
 Q_{ij} \alpha_x \int_{-h/2}^{+h/2} f_1(z) [1, z, f_1(z), f_2(z), f_1''(z), \\
 f_2''(z)] dz \\
 (C_{ij}^{T_z}, C_{sij}^{T_z}, C_{ss1ij}^{T_z}, C_{ss2ij}^{T_z}, I_{ss1ij}^{T_z}, J_{ss1ij}^{T_z}) = \\
 Q_{ij} \alpha_z \int_{-h/2}^{+h/2} f_1(z) [1, z, f_1(z), f_2(z), f_1''(z), \\
 f_2''(z)] dz \\
 (D_{ij}^{T_x}, D_{sij}^{T_x}, D_{ss1ij}^{T_x}, I_{ss2ij}^{T_x}, J_{ss2ij}^{T_x}) = \\
 Q_{ij} \alpha_x \int_{-h/2}^{+h/2} f_2(z) [1, z, f_2(z), f_1''(z), f_2''(z)] dz, \\
 (D_{ij}^{T_z}, D_{sij}^{T_z}, D_{ss1ij}^{T_z}, I_{ss2ij}^{T_z}, J_{ss2ij}^{T_z}) = \\
 Q_{ij} \alpha_z \int_{-h/2}^{+h/2} f_2(z) [1, z, f_2(z), f_1''(z), f_2''(z)] dz, \quad (A.8) \\
 (I_{ij}^{T_x}, I_{sij}^{T_x}) = Q_{ij} \alpha_x \int_{-h/2}^{+h/2} f_1''(z) [1, z] dz, \\
 (I_{ij}^{T_z}, I_{sij}^{T_z}) = Q_{ij} \alpha_z \int_{-h/2}^{+h/2} f_1''(z) [1, z] dz, \\
 (J_{ij}^{T_x}, J_{sij}^{T_x}) = Q_{ij} \alpha_x \int_{-h/2}^{+h/2} f_2''(z) [1, z, f_2''(z)] dz, \\
 (J_{ij}^{T_z}, J_{sij}^{T_z}) = Q_{ij} \alpha_z \int_{-h/2}^{+h/2} f_2''(z) [1, z, f_2''(z)] dz
 \end{aligned}$$

Moisture Coefficients

$$\begin{aligned}
 (A_{ij}^{C_x}, B_{ij}^{C_x}, A_{ij}^{C_z}) &= Q_{ij} \beta_x \int_{-h/2}^{+h/2} (1, z, z^2) dz, \\
 (A_{ij}^{C_z}, B_{ij}^{C_z}, A_{ij}^{C_x}) &= Q_{ij} \beta_z \int_{-h/2}^{+h/2} (1, z, z^2) dz, \\
 (C_{ij}^{C_x}, C_{ij}^{C_z}, C_{ss1ij}^{C_x}, C_{ss2ij}^{C_x}, I_{ss1ij}^{C_x}, J_{ss1ij}^{C_x}) \\
 &= Q_{ij} \beta_x \int_{-h/2}^{+h/2} f_1(z) [1, z, f_1(z), f_2(z), f_1''(z), \\
 &\quad f_2''(z)] dz, \\
 (C_{ij}^{C_z}, C_{ij}^{C_x}, C_{ss1ij}^{C_z}, C_{ss2ij}^{C_z}, I_{ss1ij}^{C_z}, J_{ss1ij}^{C_z}) &= \\
 Q_{ij} \beta_z \int_{-h/2}^{+h/2} f_1(z) [1, z, f_1(z), f_2(z), f_1''(z), \\
 &\quad f_2''(z)] dz, \\
 (D_{ij}^{C_x}, D_{ij}^{C_z}, D_{ss1ij}^{C_x}, I_{ss2ij}^{C_x}, J_{ss2ij}^{C_x}) &= \\
 Q_{ij} \beta_x \int_{-h/2}^{+h/2} f_2(z) [1, z, f_2(z), f_1''(z), f_2''(z)] dz, \\
 (D_{ij}^{C_z}, D_{ij}^{C_x}, D_{ss1ij}^{C_z}, I_{ss2ij}^{C_z}, J_{ss2ij}^{C_z}) &= \\
 Q_{ij} \beta_z \int_{-h/2}^{+h/2} f_2(z) [1, z, f_2(z), f_1''(z), f_2''(z)] dz, \\
 (I_{ij}^{C_x}, I_{ij}^{C_z}) &= Q_{ij} \beta_x \int_{-h/2}^{+h/2} f_1''(z) [1, z] dz, \\
 (I_{ij}^{C_z}, I_{ij}^{C_x}) &= Q_{ij} \beta_z \int_{-h/2}^{+h/2} f_1''(z) [1, z] dz, \\
 (J_{ij}^{C_x}, J_{ij}^{C_z}) &= Q_{ij} \beta_x \int_{-h/2}^{+h/2} f_2''(z) [1, z, f_2''(z)] dz, \\
 (J_{ij}^{C_z}, J_{ij}^{C_x}) &= Q_{ij} \beta_z \int_{-h/2}^{+h/2} f_2''(z) [1, z, f_2''(z)] dz
 \end{aligned} \tag{A.9}$$

Following are stiffness matrix coefficients [K] used in Eq. (13)

$$\begin{aligned}
 K_{11} &= -A_{11} \left(\frac{m^2 \pi^2}{a^2} \right), K_{12} = B_{11} \left(\frac{m^3 \pi^3}{a^3} \right), \\
 K_{13} &= -C_{11} \left(\frac{m^2 \pi^2}{a^2} \right), K_{14} = -D_{11} \left(\frac{m^2 \pi^2}{a^2} \right); \\
 K_{15} &= I_{13} \left(\frac{m\pi}{a} \right), K_{16} = J_{13} \left(\frac{m\pi}{a} \right), \\
 K_{22} &= -A_{s11} \left(\frac{m^4 \pi^4}{a^4} \right), K_{23} = C_{s11} \left(\frac{m^3 \pi^3}{a^3} \right), \\
 K_{24} &= D_{s11} \left(\frac{m^3 \pi^3}{a^3} \right), K_{25} = -I_{s13} \left(\frac{m^2 \pi^2}{a^2} \right), \\
 K_{26} &= -J_{s13} \left(\frac{m^2 \pi^2}{a^2} \right), K_{33} = -C_{ss111} \left(\frac{m^2 \pi^2}{a^2} \right) \\
 &- C_{sss155}, K_{34} = - \left[C_{ss211} \left(\frac{m^2 \pi^2}{a^2} \right) + C_{sss255} \right], \\
 K_{35} &= I_{ss113} \left(\frac{m\pi}{a} \right) - C_{sss155} \left(\frac{m\pi}{a} \right), \\
 K_{36} &= J_{ss113} \left(\frac{m\pi}{a} \right) - C_{sss255} \left(\frac{m\pi}{a} \right), \\
 K_{45} &= I_{ss213} \left(\frac{m\pi}{a} \right) - C_{sss255} \left(\frac{m\pi}{a} \right), \\
 K_{46} &= J_{ss213} \left(\frac{m\pi}{a} \right) - D_{sss155} \left(\frac{m\pi}{a} \right), \\
 K_{56} &= -C_{sss255} \left(\frac{m^2 \pi^2}{a^2} \right) - I_{sss233}, \\
 K_{66} &= -D_{sss155} \left(\frac{m^2 \pi^2}{a^2} \right) - J_{sss133}
 \end{aligned} \tag{A.10}$$

Following are force vectors used in Eq. (13)

$$\begin{aligned}
 f_{11} &= (A_{11}^T + A_{13}^T) T_{0m} \alpha + (B_{11}^T + B_{13}^T) \frac{T_{1m} \alpha}{h} \\
 &+ (C_{11}^T + C_{13}^T) \frac{T_{2m} \alpha}{h} + (D_{11}^T + D_{13}^T) \frac{T_{3m} \alpha}{h} \\
 (A_{11}^{C_z} + A_{13}^{C_z}) &C_{0m} \alpha + (B_{11}^{C_z} + B_{13}^{C_z}) \frac{C_{1m} \alpha}{h} \\
 &+ (C_{11}^{C_z} + C_{13}^{C_z}) \frac{C_{2m} \alpha}{h} + (D_{11}^{C_z} + D_{13}^{C_z}) \frac{C_{3m} \alpha}{h}
 \end{aligned} \tag{A.11}$$

$$\begin{aligned}
 f_{22} = & -q - (B_{11}^{T_x} + B_{13}^{T_z})T_{0m}\alpha^2 \\
 & - (A_{S11}^{T_x} + A_{S13}^{T_z})\frac{T_{1m}\alpha^2}{h} \\
 & - (A_{S12}^{T_x} + A_{S23}^{T_z})\frac{T_{1m}\beta^2}{h} - (C_{S11}^{T_x} + C_{S13}^{T_z})\frac{T_{2m}\alpha^2}{h} \\
 & - (D_{S11}^{T_x} + D_{S13}^{T_z})\frac{T_{3m}\alpha^2}{h} - (B_{11}^{C_x} + B_{13}^{C_z})C_{0m}\alpha^2 \\
 & - (A_{S11}^{C_x} + A_{S13}^{C_z})\frac{C_{1m}\alpha^2}{h} - (A_{S12}^{C_x} + A_{S23}^{C_z})\frac{C_{1m}\beta^2}{h} \\
 & - (C_{S11}^{C_x} + C_{S13}^{C_z})\frac{C_{2m}\alpha^2}{h} - (D_{S11}^{C_x} + D_{S13}^{C_z})\frac{C_{3m}\alpha^2}{h}
 \end{aligned} \tag{A.12}$$

$$\begin{aligned}
 f_{33} = & (C_{11}^{T_x} + C_{13}^{T_z})T_{0m}\alpha + (C_{S11}^{T_x} + C_{S13}^{T_z})\frac{T_{1m}\alpha}{h} \\
 & + (C_{SS111}^{T_x} + C_{SS113}^{T_z})\frac{T_{2m}\alpha}{h} + (C_{SS211}^{T_x} \\
 & + C_{SS213}^{T_z})\frac{T_{3m}\alpha}{h} + (C_{11}^{C_x} + C_{13}^{C_z})C_{0m}\alpha \\
 & + (C_{S11}^{C_x} + C_{S13}^{C_z})\frac{C_{1m}\alpha}{h} + (C_{SS111}^{C_x} + C_{SS113}^{C_z})\frac{C_{2m}\alpha}{h} \\
 & + (C_{SS211}^{C_x} + C_{SS213}^{C_z})\frac{C_{3m}\alpha}{h}
 \end{aligned} \tag{A.13}$$

$$\begin{aligned}
 f_{44} = & (D_{11}^{T_x} + D_{13}^{T_z})T_{0m}\alpha + (D_{S11}^{T_x} + D_{S13}^{T_z})\frac{T_{1m}\alpha}{h} \\
 & + (C_{SS211}^{T_x} + C_{SS213}^{T_z})\frac{T_{2m}\alpha}{h} (D_{SS111}^{T_x} \\
 & + D_{SS113}^{T_z})\frac{T_{3m}\alpha}{h} + (D_{11}^{C_x} + D_{13}^{C_z})C_{0m}\alpha \\
 & + (D_{S11}^{C_x} + D_{S13}^{C_z})\frac{C_{1m}\alpha}{h} + (C_{SS211}^{C_x} \\
 & + C_{SS213}^{C_z})\frac{C_{2m}\alpha}{h} + (D_{SS111}^{C_x} + D_{SS113}^{C_z})\frac{C_{3m}\alpha}{h}
 \end{aligned} \tag{A.14}$$

$$\begin{aligned}
 f_{55} = & -(I_{13}^{T_x} + I_{33}^{T_z})T_{0m} - (I_{S13}^{T_x} + I_{S33}^{T_z})\frac{T_{1m}}{h} \\
 & - (I_{SS113}^{T_x} + I_{SS133}^{T_z})\frac{T_{2m}}{h} - (I_{SS213}^{T_x} + I_{SS233}^{T_z})\frac{T_{3m}}{h} \\
 & - (I_{13}^{C_x} + I_{33}^{C_z})T_{0m} - (I_{S13}^{C_x} + I_{S33}^{C_z})\frac{T_{1m}}{h} \\
 & - (I_{SS113}^{C_x} + I_{SS133}^{C_z})\frac{C_{2m}}{h} - (I_{SS213}^{C_x} + I_{SS233}^{C_z})\frac{C_{3m}}{h}
 \end{aligned} \tag{A.15}$$

$$\begin{aligned}
 f_{66} = & -(J_{13}^{T_x} + J_{33}^{T_z})T_{0m} - (J_{S13}^{T_x} + J_{S33}^{T_z})\frac{T_{1m}}{h} \\
 & - (J_{SS113}^{T_x} + J_{SS133}^{T_z})\frac{T_{2m}}{h} - (J_{SS213}^{T_x} + J_{SS233}^{T_z})\frac{T_{3m}}{h} \\
 & - (J_{13}^{C_x} + J_{33}^{C_z})C_{0m} - (J_{S13}^{C_x} + J_{S33}^{C_z})\frac{C_{1m}}{h} \\
 & - (J_{SS113}^{C_x} + J_{SS133}^{C_z})\frac{C_{2m}}{h} - (J_{SS213}^{C_x} + J_{SS233}^{C_z})\frac{C_{3m}}{h}
 \end{aligned} \tag{A.16}$$

References

- [1] Timoshenko, S.P., Woinowsky-Krieger, S., 1959. *Theory of plates and shells*, McGraw-Hill, New York, NY.
- [2] Todhunter, I. and Person, K., 1960. *A history of the elasticity and of the strength of materials from Galileo (1564-1642) to Lord Kelvin (1824-1907)*. Vols. I, II and III, Dover Publications, New York.
- [3] Carrera, E., Guinta, G. and Petrolo, M., 2011. *Beam Structures: Classical and Advanced Theories*. John Wiley and Sons Ltd U.K.
- [4] Pagano, N. J., 1969. Exact solution for composite laminates in cylindrical bending, *Journal of Composite Materials*, 3, pp. 398-411.
- [5] Pagano, N. J., 1970. Exact solutions for bidirectional composites and sandwich plates. *Journal of Composite Materials*, 4 (1), pp. 20-34.
- [6] Pagano, N. J., 1970. Influence of shear coupling in cylindrical bending of anisotropic laminates. *Journal of Composite Materials*, 4(3), pp. 330-343.
- [7] Kirchhoff, G. R., 1850. Über das gleichgewicht und die bewegung einer elastischen scheibe, *Journal für die Reine und Angewandte Mathematik (Crelle's Journal)*, 40, pp.51-88.
- [8] Mindlin, R. D., 1951. Influence of rotary inertia and shear on flexural motions of isotropic, elastic plates. *Journal of Applied Mechanics*, 18, pp. 31-38.
- [9] Sayyad, A. S., 2011. Comparison of various refined beam theories for the bending and free vibration analysis of thick beams. *Applied and Computational Mechanics*, 5, pp. 217-230.
- [10] Sayyad, A. S. and Ghugal, Y. M., 2012. Bending and free vibration analysis of thick isotropic plates by using exponential shear deformation theory. *Applied and Computational Mechanics*, 6, pp. 65-82.
- [11] Sayyad, A. S. and Ghugal, Y. M., 2012. Buckling analysis of thick isotropic plates by using exponential shear deformation theory. *Applied and Computational Mechanics*, 6, pp. 185-196.
- [12] Ghugal, Y. M. and Dahake, A. G., 2012. Flexural analysis of deep beam subjected to parabolic load using refined shear deformation theory, *Applied and Computational Mechanics*, 6, pp. 163-172.
- [13] Sayyad, A. S. and Ghugal, Y. M., 2015. Static flexure of soft-core sandwich beams using trigonometric shear deformation theory, *Mechanics of Advanced Composite Structures*, 2, pp. 45-53.

- [14] Sayyad, A.S. and Ghugal, Y. M., 2015. A nth order shear deformation theory for composite laminates in cylindrical bending. *Curved and Layered Structures*, 2, pp. 290-300.
- [15] Sayyad, A. S. and Ghugal, Y. M., 2016. Single variable refined beam theories for the bending, buckling and free vibration of homogeneous beams. *Applied and Computational Mechanics*, 10, pp. 123-138.
- [16] Shinde, B. M. and Sayyad, A. S., 2017. A quasi-3D polynomial shear and normal deformation theory for laminated composite, sandwich and functionally graded beams. *Mechanics of Advanced Composite Structures*, 4, pp. 139-152.
- [17] Sayyad, A. S. and Ghugal, Y. M., 2018. Bending, buckling and free vibration responses of hyperbolic shear deformable FGM beams, *Mechanics of Advanced Composite Structures*, 5, pp. 13-24.
- [18] Sayyad, A. S. and Naik, N. S. 2019. New displacement model for accurate prediction of transverse shear stresses in laminated and sandwich rectangular plates. *ASCE Journal of Aerospace Engineering*, 32(5), pp. 1-12.
- [19] Plucinski, P. and Jaskoweich J., 2020. Three-Dimensional Analysis of Laminated Plates with functionally graded layers by two-dimensional numerical model. *Engineering Transactions*, 68(1), pp. 21-45.
- [20] Sayyad, A. S. and Ghugal, Y. M., 2015. On the free vibration analysis of laminated composite and sandwich plates: A review of recent literature with some numerical results. *Composite Structures*, 129, pp. 177-201.
- [21] Sayyad, A. S. and Ghugal, Y. M., 2017. Bending, buckling and free vibration of laminated composite and sandwich beams: A critical review of literature. *Composite Structures*, 171, pp. 486-504.
- [22] Sayyad, A. S. and Ghugal, Y. M., 2019. Modelling and analysis of functionally graded sandwich beams: A Review. *Mechanics of Advanced Materials and Structures*, 26 (21), pp. 1776-1795.
- [23] Cho, K. N., Striz, A. G. and Bert, C. W., 1989. Thermal stress analysis of laminate using higher-order theory in each layer. *Journal of Thermal Stresses*, 12(3), pp. 321-332.
- [24] Bhaskar, K., Varadan, T. K. and Ali, J. S. M., 1996. Thermoelastic solutions for orthotropic and anisotropic composite laminates, *Composites part B*, 27B, pp. 415-420.
- [25] Carrera, E., 2000. An assessment of mixed and classical theories for the thermal stress analysis of orthotropic multilayered plates, *Journal of thermal stresses*, 23, pp. 797-831.
- [26] Rohwer K., Rolles R. and Sparr H., 2001. Higher-order theories for thermal stresses in layered plates. *International Journal of Solids and Structures*, 38 (21), pp. 3673-3687.
- [27] Robaldo, A. and Carrera, E., 2007. Mixed finite elements for thermoelastic analysis of multilayered anisotropic plates. *Journal of Thermal Stresses*, 30(2), pp. 165-194.
- [28] Kant, T. and Shiyekar, S. M., 2013. An assessment of a higher order theory for composite laminates subjected to thermal gradient. *Composite Structures*, 96, pp. 698-707.
- [29] Sayyad, A. S., Ghugal, Y. M. and Mhaske, B. A., 2015. A four-variable plate theory for thermoelastic bending analysis of laminated composite plates. *Journal of Thermal Stresses*, 38, pp. 904-925.
- [30] Sayyad, A. S., Ghugal, Y. M. and Shinde, B. M., 2016. Thermal stress analysis of laminated composite plates using exponential shear deformation theory. *International Journal of Automotive Composites*, 2(1), pp. 23-40.
- [31] Zenkour, A. M. and Radwan, A. F., 2017. Analysis of multilayered composite plates resting on elastic foundations in thermal environment using hyperbolic model. *Journal of the Brazilian Society of Mechanical Sciences and Engineering*, 39(7), pp. 2801-2816.
- [32] Shaharavi, M., Fallahzade, S. and Mokhtari, M., 2018. An analytical approach to thermo elastic bending of simply supported advanced ribbed composite plates. *Mechanics of Advanced Composite Structures*, 5, pp. 173-185.
- [33] Evran, S., 2019. Finite element analysis of thermal stress of laminated composite plates using Taguchi method. *Manas Journal of Engineering*, 7(2), pp. 121-125.
- [34] Carrera, E. and Nali, P., 2010. Multilayered plate elements for the analysis of multi-field problems. *Finite Elements in Analysis and Design*, 46, pp. 732-742.
- [35] Ali, J. S. M., Bhaskar, K. and Varadan, T. K., 1999. A new theory for accurate thermal/mechanical flexural analysis of symmetric laminated plates, *Composite structures*, 45, pp. 227-232.
- [36] Zenkour, A. M., 2004. Analytical solution for bending of cross-ply laminated plates under thermomechanical loading. *Composite Structures*, 65(3-4), pp. 367-379.

- [37] Kant, T., Pendhari, S. S. and Desai, Y. M., 2008. An efficient semi-analytical model for composite and sandwich plates subjected to thermal load. *Journal of Thermal Stresses*, 31 pp. 77-103.
- [38] Nali, P. and Carrera, E., 2013. Accurate buckling analysis of composite layered plates with combined thermal and mechanical loadings. *Journal of Thermal Stresses*, 36(1), pp. 1-18.
- [39] Wu, Z., Lo, S. H. and Sze, K. Y., 2013. Influence of transverse normal strain and temperature profile on thermoelasticity of sandwiches in terms of the enhanced Reddy's theory. *Journal of Thermal Stresses*, 36(1), pp. 19-36.
- [40] Ghugal, Y. M. and Kulkarni, S. K., 2013. Flexural analysis of cross-ply laminated plates subjected to nonlinear thermal and mechanical loadings. *Acta Mechanica*, 224(3), pp. 675-690.
- [41] Ghugal, Y. M. and Kulkarni S. K., 2013. Thermal flexural analysis of cross-ply laminated plates using trigonometric shear deformation theory. *Latin American Journal of Solids and Structures*, 10, pp. 1001-1023.
- [42] Zenkour, A. M., Allam, M. N. M. and Radwan, A. F., 2013. Bending of cross-ply laminated plates resting on elastic foundations under thermo-mechanical loading. *International Journal of Mechanics and Materials in Design*, 9 (3), pp. 239-251.
- [43] Wu, Z. and Xiaohui, R., 2017. Thermomechanical analysis of multilayered plates in terms of Reddy-type higher-order theory. *Mechanics of Advanced Materials and Structures*, 24 (14), pp. 1196-1205.
- [44] Patel, B. P., Ganapathi M. and Makhecha D. P., 2002. Hygrothermal effects on the structural behavior of thick composite laminates using higher-order theory. *Composite Structures*, 56 (1), pp.25-34.
- [45] Zenkour, A. M., 2012. Hygrothermal effects on the bending of angle-ply composite plates using a sinusoidal theory. *Composite Structures*, 94 (12), pp. 3685-3696.
- [46] Wu, Z. and Lo, S. H., 2015. Hygrothermomechanical effects on laminated composite plates in terms of a higher-order global-local model. *Journal of Thermal Stresses*, 38(5), pp. 543-568.
- [47] Najafi, M., Ansari, R. and Darvizeh, A., 2017. Environmental effects on mechanical properties of glass/epoxy and fiber metal laminates, Part-I: Hygrothermal aging. *Mechanics of Advanced Composite Structures*, 4, pp. 187-196.
- [48] Najafi, M., Ansari, R. and Darvizeh, A., 2017. Environmental effects on mechanical properties of glass/epoxy and fiber metal laminates, Part-II: Isothermal aging. *Mechanics of Advanced Composite Structures*, 4, pp. 197-205.
- [49] Akbas, S. D., 2019. Nonlinear static analysis of laminated composite beams under hygrothermal effect. *Structural Engineering and Mechanics*, 72(4), pp. 433-441.
- [50] Sayyad, A. S. and Ghugal, Y. M., 2019. Effects of nonlinear hygrothermomechanical loading on bending of FGM rectangular plates resting on two-parameter elastic foundation using four-unknown theory. *Journal of Thermal Stresses*, 42 (2), pp.213-232.
- [51] Zenkour, A. M. and Radwan, A. F. 2019. Hygrothermo-mechanical buckling of FGM plates resting on elastic foundations using a quasi-3D model. *International Journal for Computational Methods in Engineering Science and Mechanics*, 20(2), pp.85-98.
- [52] Garg, A. and Chalak, H. D., 2019. A review on analysis of laminated composites and sandwich structures under hygrothermal conditions. *Thin Walled Structures*, 142, pp. 202-226.
- [53] Moleiro, F., Mota Soares, G.M. and Carrera, E., 2019. Three-dimensional exact hygrothermoelastic solutions for multilayered plates composite laminates, fibre metal laminates and sandwich plates. *Composite Structures*, 216, pp. 260-278.
- [54] Das, A. and Niyogi, A. G., 2020. Free-vibration analysis of epoxy-based cross-ply laminated composite folded plates subjected to hygrothermal loading. *Journal of Institute of Engineers (India) Series C*, pp. 1-17.
- [55] Naik, N. S. and Sayyad, A. S., 2020. Analysis of laminated plates subjected to mechanical and hygrothermal environmental loads using fifth-order shear and normal deformation theory. *International Journal of Applied Mechanics*, 12(3), pp. 1-51.
- [56] Naik, N. S. and Sayyad, A. S., 2018. 1D analysis of laminated composite and sandwich plates using a new fifth-order plate theory. *Latin American Journal of Solids and Structures*, 15(1), pp. 1-17.
- [57] Naik, N. S. and Sayyad, A. S., 2018. 2D analysis of laminated composite and sandwich plates using a new fifth-order plate theory. *Latin American Journal of Solids and Structures*, 15 (9), pp.1-27.
- [58] Naik, N. S. and Sayyad, A. S., 2019. An accurate computational model for thermal analysis of laminated composite and sandwich plates. *Journal of Thermal Stresses*, 42 (5), pp. 559-579.
- [59] Ghumare, S. M. and Sayyad, A. S., 2017. A new fifth-order shear and normal deformation theory for static bending and elastic buckling

- of P-FGM beams. *Latin American Journal of Solids and Structures*, 14(5), pp. 1893-1911.
- [60] Ghumare, S. M. and Sayyad, A. S., 2019. A new quasi-3D model for functionally graded plates. *Journal of Applied and Computational Mechanics*, 5(2), pp. 367-380.
- [61] Ghumare, S. M. and Sayyad, A. S. 2019. Nonlinear hygro-thermo-mechanical analysis of functionally graded plates using a fifth-order plate theory. *Arabian Journal for Science and Engineering*, DOI: 10.1007/513369-019-03894-8.
- [62] Carrera, E., 2005. Transverse normal strain effects on thermal stress analysis of homogeneous and layered plates, *AIAA journal*, 43(10), pp. 2232-2242.
- [63] Reddy, J. N., 1984. A simple higher-order theory for laminated composite plates. *Journal of Applied Mechanics*, 51(4), pp. 745-752.
- [64] Kant, T. and Swaminathan, K., 2000. Analytical solutions for the static analysis of laminated composite and sandwich plates based on a higher order refined theory. *Composite Structures*, 56, pp. 329-344.
- [65] Kapuria, S., Dumir, P. C. and Jain, N. K., 2004. Assessment of zigzag theory for static loading, buckling, free and forced response of composite and sandwich beams. *Composite Structures*, 64, pp. 317-327.
- [66] Sayyad, A. s. and Ghugal, Y. M., 2016. Cylindrical bending of multilayered composite laminates and sandwiches. *Advances in Aircraft and Spacecraft sciences*, 3 (2), pp. 113-148.